MIT Libraries | DSpace@MIT

MIT Open Access Articles

Importance of aerosol composition, mixing state, and morphology for heterogeneous ice nucleation: A combined field and laboratory approach

Massachusetts Institute of Technology

Importance of aerosol composition, mixing state, and morphology for heterogeneous ice nucleation: A combined field and laboratory approach

Kelly J. Baustian,[1,2] Daniel J. Cziczo,[3,4] Matthew E. Wise,[1,5] Kerri A. Pratt,[3,6] Gourihar Kulkarni,[3] A. Gannet Hallar,[7] and Margaret A. Tolbert[1,8]

[1]   In this study chemical compositions of background aerosol and ice nuclei were examined through laboratory investigations using Raman spectroscopy and field measurements by single-particle mass spectrometry. Aerosol sampling took place at Storm Peak Laboratory in Steamboat Springs, Colorado (elevation of 3210 m). A cascade impactor was used to collect coarse-mode aerosol particles for laboratory analysis by Raman spectroscopy; the composition, mixing state, and heterogeneous ice nucleation activity of individual particles were examined. For in situ analysis of fine-mode aerosol, ice nucleation on ambient particles was observed using a compact ice nucleation chamber. Ice crystals were separated from unactivated aerosol using a pumped counterflow virtual impactor, and ice nuclei were analyzed using particle analysis by laser mass spectrometry. For both fine and coarse modes, the ice nucleating particle fractions were enriched in minerals and depleted in sulfates and nitrates, compared to the background aerosol sampled. The vast majority of particles in both the ambient and ice active aerosol fractions contained a detectable amount of organic material. Raman spectroscopy showed that organic material is sometimes present in the form of a coating on the surface of inorganic particles. We find that some organic-containing particles serve as efficient ice nuclei while others do not. For coarse-mode aerosol, organic particles were only observed to initiate ice formation when oxygen signatures were also present in their spectra.

Citation: Baustian, K. J., D. J. Cziczo, M. E. Wise, K. A. Pratt, G. Kulkarni, A. G. Hallar, and M. A. Tolbert (2012), Importance of aerosol composition, mixing state, and morphology for heterogeneous ice nucleation: A combined field and laboratory approach, *J. Geophys. Res.*, *117*, D06217, doi:10.1029/2011JD016784.

1.   Introduction

[2]   Ice cloud formation remains one of the least understood processes in our atmosphere and one of the most uncertain aspects of climate change [*Intergovernmental Panel on Climate Change*, 2007]. In cirrus clouds, ice crystals develop on or in aerosol particles, termed ice nuclei (IN), which serve as surfaces for ice formation. The ice-forming activity of complex atmospheric aerosol particles with varying composition, mixing state and morphology is difficult to predict. To explain the complex interplay between aerosol composition and ice cloud formation, we must characterize the nature of particles that serve as IN. This includes collecting information about IN size, shape, phase, mixing state and chemical constituents. Because ice formation occurs on or in ambient aerosol particles, changes in aerosol composition due to natural and anthropogenic pollutant sources may also affect atmospheric cloud formation and therefore global climate.

[3]   Tropospheric cirrus cloud formation is known to proceed via multiple mechanisms which have not been fully elucidated [*Cantrell and Heymsfield*, 2005; *Pruppacher and Klett*, 1997]. Ice nucleation mechanisms have been divided into two primary categories, homogeneous and heterogeneous nucleation. Homogeneous ice nucleation occurs when an ice germ forms within the aqueous matrix of a supercooled liquid particle, initiating spontaneous freezing of the entire droplet. Solutes have been shown to depress the freezing point temperature necessary for homogeneous ice formation below that of pure water [*Koop et al.*, 2000]. Heterogeneous ice formation requires a surface to initiate ice

[1]Cooperative Institute for Research in Environmental Sciences, University of Colorado Boulder, Boulder, Colorado, USA.
[2]Department of Atmospheric and Oceanic Science, University of Colorado Boulder, Boulder, Colorado, USA.
[3]Pacific Northwest National Laboratory, Richland, Washington, USA.
[4]Now at Department of Earth, Atmospheric and Planetary Sciences, Massachusetts Institute of Technology, Cambridge, Massachusetts, USA.
[5]Now at Department of Chemistry, Concordia University, Portland, Oregon, USA.
[6]Now at Department of Chemistry, Purdue University, West Lafayette, Indiana, USA.
[7]Storm Peak Laboratory, Desert Research Institute, Steamboat Springs, Colorado, USA.
[8]Department of Chemistry and Biochemistry, University of Colorado Boulder, Boulder, Colorado, USA.

nucleation. Particles serving as heterogeneous IN have surface properties that lower the energy barrier for ice formation. If present, heterogeneous IN can initiate ice nucleation at warmer temperatures ($>-37°C$) and lower supersaturation with respect to ice than required for homogeneous freezing. The abundance of atmospheric IN (on the order of tens per liter) typically limits heterogeneous ice formation to very low number concentrations [*DeMott et al.*, 2003].

[4] Depending on aerosol phase and in-cloud dynamics, ice formation may proceed via multiple pathways within a single cloud. Modeling studies documenting the competition between heterogeneous and homogeneous ice nucleation mechanisms have a history that dates back more than 20 years [*DeMott et al.*, 1997; *Gierens*, 2003; *Kärcher*, 2005; *Ren and Mackenzie*, 2005; *Spichtinger and Gierens*, 2009a, 2009b, 2009c]. Recent studies [e.g., *Kamphus et al.*, 2010; *Spichtinger and Cziczo*, 2010] highlight some unresolved questions regarding heterogeneous ice nucleation. Results from *Spichtinger and Cziczo* [2010] indicate ice formation initiated at low levels of supersaturation by heterogeneous IN may in turn affect homogeneous ice formation that occurs once higher supersaturation levels are achieved. They emphasize that additional information regarding how aerosol type, temperature and IN size affect heterogeneous nucleation is necessary to reduce error in model outputs. *Kamphus et al.* [2010] also stress the need for more specific information regarding the physical and chemical properties, state of mixing, and influence of possible surface coatings on IN particles. In order to constrain heterogeneous ice nucleation in models it is essential that supersaturation, IN number concentration, particle composition and size be measured accurately. *DeMott et al.* [2010] suggests heterogeneous IN concentration in models can be related to total aerosol number concentration of particles larger than 0.5 μm in diameter. Thus, it is possible to develop simple parameterizations that can be incorporated into models for estimating ice concentrations based on investigation of large particles that are important for ice nucleation. This work also acknowledges a composition effect that is not fully modeled and may account for much of the remaining uncertainty in ice number concentrations.

[5] This study is designed to investigate how physical and chemical properties of aerosol particles influence ice formation in the heterogeneous freezing regime at temperatures relevant for cirrus cloud formation. Since heterogeneous ice nucleation occurs on only a very small subset of ambient particles, single particle analysis is important for establishing complete understanding of the underlying mechanism(s). The use of Raman microspectroscopy has become increasingly recognized as a valuable tool for studying individual aerosol particles. This effort was pioneered by Rosasco and Blaha and advanced by Fung and Tang [e.g., *Blaha and Rosasco*, 1978; *Fung and Tang*, 1992, 1999; *Rosasco et al.*, 1975; *Tang and Fung*, 1989] *Yeung and Chan*, 2010]. Raman spectroscopy is well suited for the study of aerosol particles because it provides a nondestructive way to identify chemical components present within individual particles and ascertain how they are distributed relative to one another. More common techniques for single-particle aerosol investigation, such as transmission electron microscopy (TEM), may damage the particles and require vacuum conditions that may evaporate semivolatile species [*Freedman et al.*,

2010]. The spatial resolution of the Raman spectrometer makes it possible to probe individual micron-sized particles; resulting vibrational spectra are highly specific and allow for identification of chemical functional groups. Minor chemical constituents can often be identified as well. From these spectra, information about particle composition, mixing state, phase and particle origin may be determined. Several groups have demonstrated the utility of Raman spectroscopy for investigating the composition of ambient aerosol samples collected from the atmosphere [*Batonneau et al.*, 2006; *Deboudt et al.*, 2010; *Guedes et al.*, 2009; *Ivleva et al.*, 2007; *Potgieter-Vermaak and Van Grieken*, 2006; *Sobanska et al.*, 2006; *Uzu et al.*, 2009].

[6] Only a few studies have used Raman spectroscopy to investigate ice nucleation [*Baustian et al.*, 2010; *Knopf and Koop*, 2006; *Mund and Zellner*, 2003; *Wise et al.*, 2010]. These studies are all based on investigation of laboratory-generated samples. Here we use Raman spectroscopy to probe heterogeneous ice nucleation on collected ambient aerosol particles. Particles were collected at a high-altitude research site (Storm Peak Laboratory) located in the Rocky Mountains of Northwest Colorado. Concurrent measurements of aerosol and heterogeneous IN composition were also made using single particle mass spectrometry, a technique used previously to examine the chemistry of IN at Storm Peak Laboratory [*Cziczo et al.*, 2006; *DeMott et al.*, 2003; *Richardson et al.*, 2007]. The present study represents the first attempt to study ice nucleation on ambient aerosol particles using Raman spectroscopy and demonstrates this technique can provide detailed information about ice nucleation at the single-particle level.

2. Experimental Methods and Sampling

2.1. Field Campaign

[7] Air sampling was conducted in January 2010 at DRI's Storm Peak Laboratory, located at 3210 m in Northwestern Colorado (106.74°W, 40.45°N) [*Borys and Wetzel*, 1997]. The mountain top research facility is uniquely situated for conducting studies of aerosol-cloud interactions given that it is frequently above cloud base, often allows for sampling of free tropospheric air and generally has a clear upwind fetch. Throughout the campaign ambient temperature, pressure, relative humidity, and other standard meteorological variables were continuously monitored.

2.2. Raman Analysis
2.2.1. Coarse-Mode Particle Collection

[8] Aerosol particles for Raman spectroscopic analysis were collected on quartz substrates using a fixed-plate cascade impactor operating in cloud-free conditions at a flow rate of 4 L/min. A single impactor stage, with a 50% cutoff diameter of ~2 μm was used for coarse-mode particle collection. The impactor was operated in an inverted manner to prevent debris from contaminating the sample. The impactor's cutoff diameter provided only a lower bound for aerosol size, therefore optical microscopy was used to carefully count every particle and calculate average particle size. A mosaic of optical microscope images recorded at 50× magnification was used to exam the entire sample and allowed for systematic counting, measuring and spectral analysis of particles. This method was also used to ensure

that particles examined were not duplicates. Mean particle size was 4.0 ± 1.5 μm aerodynamic diameter and 95% of the particles were between 1 and 7 μm.

[9] Collected particles were ≥ 1 μm aerodynamic diameter; defined here as coarse-mode particulate. Previous measurements of heterogeneous IN suggest that most are >0.5 μm in diameter [*Cziczo et al.*, 2006; *DeMott et al.*, 2010]. Further, *Santachiara et al.* [2010] reported that particles ≤ 1 μm in diameter account of $\sim$50% of ambient IN concentration and particles less than 10 μm in diameter account for 70%–90% of ambient IN concentrations. The size range of coarse-mode particulate examined in the present study is therefore atmospherically relevant, and includes a portion of particles in the typical size range for ambient heterogeneous IN particles. Dust particles, which have previously been observed at Storm Peak Laboratory [*Hallar et al.*, 2011; *Obrist et al.*, 2008], considered to be effective IN [*Cziczo et al.*, 2004; *DeMott et al.*, 2003], are also often present in the coarse-mode aerosol. Results presented here are from laboratory-based experiments conducted using a single coarse-mode sample that was collected with simultaneous measurements of fine-mode particulate by single particle mass spectrometry.

2.2.2. Raman Microspectroscopy and Environmental Cell

[10] The Raman system used for analysis of coarse-mode particles consists of a Niclolet Almega XR Dispersive Raman microscope that has been coupled to a Buck Research CR-1A chilled-mirror hygrometer and a modified Linkam THMS600 environmental cell. The spectrometer also includes an Olympus optical microscope with $10\times$, $20\times$, $50\times$ and $100\times$ magnification capabilities. This setup, including modifications and calibrations, has been previously described in detail by *Baustian et al.* [2010].

[11] In the present study, both individual spectra and spectral maps were acquired in a point-by-point manner. A frequency doubled Nd:YVO$_4$ DPSS laser operating at 532 nm was used for molecular excitation. Spectra were obtained using $50\times$ and $100\times$ microscope objectives which have laser spot sizes similar to the diffraction limited spatial resolution of the optical microscope, about 1 μm in diameter. Between 12 and 128 exposures of 0.5 s each were averaged to generate the individual spectra presented in this study. Laser power was kept as low as possible to prevent damage to the sample. Laser damage was easily detected using both visual inspection and spectral changes. In the event that laser damage did occur, the particle was deemed of unknown composition.

[12] Raman mapping was used to gather information about the spatial distribution of chemicals within individual particles of interest. Two dimensional spectral maps were created by gathering individual spectra in 1 μm steps over the entire XY plane of single particles. The $50\times$ or $100\times$ microscope objectives were utilized along with an automated mapping program and high-precision motorized stage to ensure accurate particle mapping. Individual spectra were used for aerosol identification while spectral maps were used to characterize the spatial distribution of chemical species within particles of interest. An automated smoothing routine that employs linear pixel averaging was used to create spectral maps from individual spectra. Because of their relatively low resolution, these maps were not used as a

quantitative means for determining chemical abundances, but rather a qualitative depiction of the distribution of chemical species within particles of interest.

2.2.3. Raman Spectral Classification

[13] Raman spectra that exhibited similar physical and chemical traits were binned into groups according to the presence of characteristic Raman frequencies. The vast majority ($>90\%$) of the spectra obtained in this study exhibited characteristic frequencies associated with one or more of the following chemical functional groups: hydrocarbons, sulfates, nitrates, mineral carbonates, ammonium, and hydroxyl. Characteristic bands for these functional groups are shown in Figure 1. One additional category, "other," was necessary for classification of particles lacking distinctive spectral features necessary for identification (including those that suffered damage from the laser or those that were highly fluorescent). Particles categorized as "other" made up $6\% \pm 2\%$ of the background aerosol sampled. Raman frequencies used to assign particle composition were determined using common references, databases, literature and verified by examining chemical standards using our Raman system [*Baranska et al.*, 1987; *Batonneau et al.*, 2006; *Coleyshaw et al.*, 2003; *Ivleva et al.*, 2007; *Lin-Vien et al.*, 1991; *Mikkelsen et al.*, 1999; *Nyquist et al.*, 1997; *Potgieter-Vermaak and Van Grieken*, 2006; *Sadezky et al.*, 2005; *Tang and Fung*, 1989].

[14] The majority of Raman spectra obtained from ambient aerosol particles exhibited some degree of fluorescence. This is typically due to the presence of complex organic material with conjugated double bonds, biological material, soot or a class of organic molecules termed humiclike substances (HULIS) [*Ivleva et al.*, 2007]. The degree of fluorescence observed in this study was highly variable and included a fraction of spectra that exhibited such a high degree of fluorescence that the CCD detector was saturated. Such particles were placed in the category "other" since no specific molecular information could be obtained.

2.2.4. Heterogeneous Ice Nucleation Experiments

[15] Raman analysis was used to investigate ice nucleation on the collected coarse-mode sample. A series of heterogeneous ice nucleation experiments were performed at temperatures ranging from 210 to 230 K. For each experiment, cell temperature was held constant and RH with respect to water (starting with $\sim$0%) was increased slowly until the presence of ice was detected using optical microscopy. Selective ice nucleation events were used to identify single micron-sized IN particles and Raman spectroscopy was used to probe their composition. For each experiment, RH was increased at a relative rate of humidity change between 1% and 10% per min. To ensure that ice preactivation did not influence results, for repeated freezing experiments, the sample was warmed to 298 K and dried to 0% RH before the next experiment was initiated.

[16] Individual ice nucleation events were quantified by calculating water vapor saturation ratios relative to ice (S_{ice}) as a function of temperature observed at the onset of each heterogeneous ice nucleation event. S_{ice} is a ratio of the water partial pressure to the equilibrium vapor pressure of water over ice ($S_{ice}(T) = P_{H2O}/VP_{ice}(T)$). P_{H2O} is determined from frost point values measured by the hygrometer, which are converted to partial pressures using formulations developed by *Buck* [1981]. $VP_{ice}(T)$ is calculated using the vapor
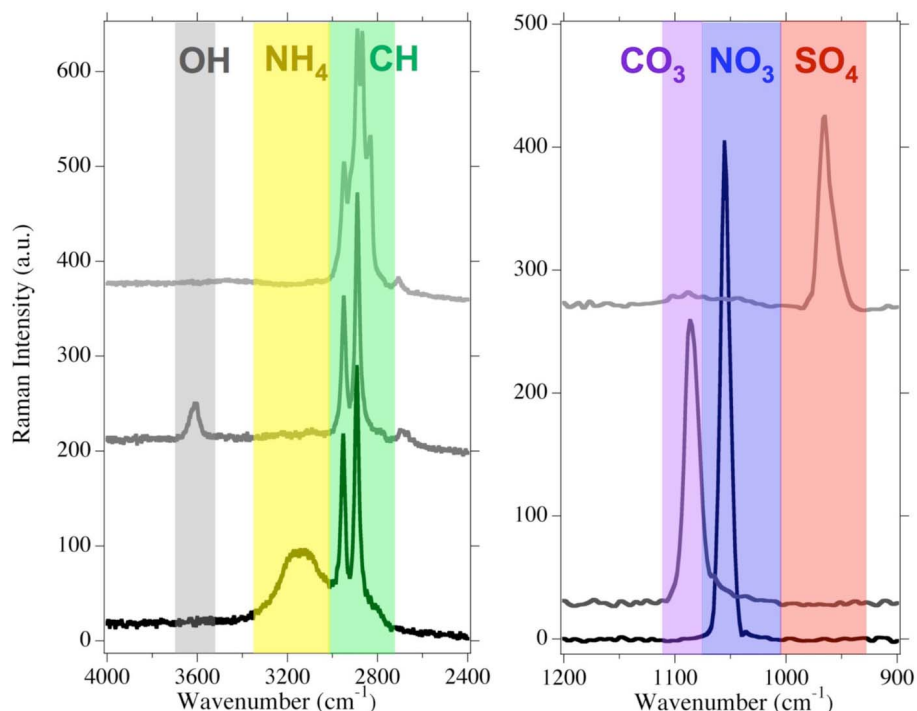
Figure 1. Characteristic Raman vibrational frequencies of six functional groups commonly associated with spectra obtained in this study. Spectra were binned into groups according to the following spectral ranges: sulfates, sharp peak between 972 and 1008 cm^{-1}; nitrates, sharp peak 1032 and 1069 cm^{-1}; carbonates, 1070–1090 cm^{-1}; C-H vibrations indicative of organic material, 2800–3000 cm^{-1}; ammonium, broad peak 3200–3400 cm^{-1}; hydroxyl, 3250–3650 cm^{-1}.

pressure formulations of *Marti and Mauersberger* [1993] and calibrated cell temperature. The largest source of experimental uncertainty in this calculation comes from uncertainty in the temperature calibration [*Baustian et al.*, 2010] of the environmental cell. Uncertainties listed for S_{ice} values reflect ± one standard deviation of uncertainty in this temperature calibration. S_{ice} values were used to quantify the onset of ice nucleation for each experiment in this study. Ice nucleation experiments on blank quartz substrates were also performed to ensure substrate effects did not influence results. The onset of ice formation was not observed on blank substrates until $S_{ice} \geq 1.8$.

2.3. PALMS Instrument and Ice Chamber

[17] Ambient cloud-free air was sampled at 10 L/min using a quasi-isokinetic inlet with an inline impactor. The cyclone impactor was operated at a 50% cut point of 1 μm. Because of the cut point, particles up to 2 μm were observed. In situ analysis of background aerosol and subsequent ice residue chemical composition were sampled in two types of experiments. First, to characterize the background ambient aerosol, the chemistry of individual particles was measured using single-particle mass spectrometry. Second, to determine the chemistry of ice-nucleating particles, cloud-free air was directed into an ice chamber to nucleate ice at specific temperature and RH conditions. Ice crystals were selected using a pumped counterflow virtual impactor (PCVI) and analyzed via single-particle mass spectrometry, similar to experiments by *Cziczo et al.* [2003].

[18] Ice nucleation experiments were conducted using a compact ice nucleation chamber (CIC) [*Friedman et al.*, 2011], that is based on the design of *Stetzer et al.* [2008] and similar to the portable ice nucleation chamber (PINC) described by *Chou et al.* [2011]. Instrumental principles, ice crystal residence time and growth have been previously described in detail by *Friedman et al.* [2011], *Stetzer et al.* [2008], and *Chou et al.* [2011]. In the CIC, water vapor diffusion between two ice-coated surfaces, held at different temperatures, created a supersaturated environment through which the aerosol flow passed. Here particles were exposed to temperature and saturation ratios representative of conditions responsible for heterogeneous ice formation in the upper troposphere (T = 230 ± 1 K and S_{ice} = 1.4 ± 0.05). Ice particles were detected by an optical particle counter at the outlet of the CIC.

[19] Output flow from the CIC was directed into an evaporation region held near ice saturation. In this section, water droplets evaporated and were removed, whereas, ice crystal size was maintained. Data collected during times when RH in the evaporation region exceeded 100% with respect to liquid water, where droplets may be confused with ice crystals, were not used in these analyses. The flow was then sent into a PCVI [*Kulkarni et al.*, 2011] with a 50% cut point of ∼3 μm, so that ice crystals were separated from unactivated aerosol and droplet residuals. Inside the PCVI a counterflow of dry N_2 was used to remove any condensed phase water, allowing the remaining ice crystal residuals, hereafter termed IN, to be sampled by single-particle mass spectrometry.

[20] Mass spectra and size distributions of background and ice active particles were gathered using particle analysis by laser mass spectrometry (PALMS) [*Cziczo et al.*, 2006]. Aerosol particles, drawn into PALMS using differential pumping stages, were detected and sized according to their aerodynamic diameter by two continuous visible laser beams (532 nm) set a known distance apart. Particles were subsequently ablated and the components ionized using a pulsed UV (193 nm) laser. The single-particle mass spectra were detected with a time of flight reflectron mass spectrometer. In this study, mass spectra collected provide a qualitative depiction of the aerosol on a particle-by-particle basis. Negative ion mass spectra often contained fragments of sulfates, nitrates, organics, and chlorine-containing species. Generally, positive ion mass spectra contained metallic components of mineral and anthropogenic origin, potassium from mineral dust and biomass burning, sulfate and organic fragments. Particles observed using PALMS were grouped into spectrally similar categories. Positive ion categories, following the method outlined by *DeMott et al.* [2003], are sulfate-organic mixtures, potassium- and carbon-containing particles (i.e., biomass burning), mineral dust, elemental carbon/vanadium (fuel combustion), and metallic particles.

[21] Several experimental artifacts have been taken in to account during the collection and processing of data from the CIC/PALMS. Infrequent frost events from the CIC were identified by sharp increases in ice crystal counts. In some more intense frost events, bursts of aluminum and stainless steel particles from large ice crystals interacting with the PCVI and other components [*Cziczo et al.*, 2003] were observed in mass spectra. Frost counts have been subtracted from the IN concentration data and associated artifact metallic particles were subtracted from the mass spectrometry data presented here. Approximately 1% of IN mass spectra may correspond to non-IN particles that were unintentionally transmitted through the PCVI [*Pekour and Cziczo*, 2011]. This experimental artifact has been included within errors reported for all mass spectral results. Periodic use of an inline filter was also used to determine the magnitude of background artifacts on the optical particle counter [*Friedman et al.*, 2011]. They were on the order of 10 per liter and have also been subtracted from the data.

[22] Technical differences between the Raman and PALMS instruments led to differences in the information provided by their spectra and the size of particulate matter examined. Raman spectroscopy gives bonding information for stable species via vibrational spectroscopy without breaking chemical bonds. In contrast, PALMS uses an excimer laser to vaporize particles and ionize molecules for analysis by mass spectrometry. Thus, different chemical information is obtained from the two techniques. However, data gathered from these two instruments can be used for complementary analysis. While PALMS and the CIC allow for in situ analysis of a large number of particles, information on the spatial variation of chemical constituents, functional groups and morphology of the single particles is available from the Raman analysis. PALMS can gather chemical information on particles smaller than the detection limit for Raman spectroscopy, whereas the Raman spectrometer can examine aerosol of sizes >2 μm that were not sampled by PALMS. Results from both single-particle techniques are qualitative in nature. For this reason, we report only the presence or absence chemical species and do not attempt to quantify relative chemical abundances.

3. Results and Discussion

3.1. Aerosol Sampling, Air Mass Transport, and Conditioning

[23] The coarse-mode sample for Raman analysis was collected from 03:35 to 09:37 local time (LT) on 26 January 2010 and contained 2162 particles equal to or larger than 0.5 μm in diameter. Particles did not appear to agglomerate on the substrate, they were deposited well separated from one another in a circle ~1 mm in diameter. The average particle size for the sample was 4.0 ± 1.5 μm. From 01:37 to 02:03 LT and 04:16 to 05:20 LT on 26 January 2010, PALMS was used to gather 3840 mass spectra of ambient particles in positive and negative polarity modes. During the intermediate period (02:27–03:22 LT), PALMS was attached to the CIC via the PCVI to characterize the subset of particles that heterogeneously nucleated ice. In total, positive ion mass spectra of 204 IN were collected using the PALMS/CIC.

[24] Backtrajectories of air parcel history, transport and RH environment of the sampled air mass were created using NOAA's Hybrid Single-Particle Lagrangian Integrated Trajectory model (HYSPLIT) (R. R. Draxler and G. D. Rolph, HYSPLIT, http://www.arl.noaa.gov/HYSPLIT_info. php; READY, http://ready.arl.noaa.gov/). NCEP/NCAR reanalysis data from January 2010 was used to create HYSLPIT modeled outputs. From the ending location of Storm Peak Laboratory at 3210 m, predicted air mass back trajectories were generated for 48 h prior to the end of aerosol sampling. HYSPLIT trajectories indicate that sampled particles originated from the regions west of Storm Peak Laboratory. 48 h prior to sampling, the air mass was at low elevations (~500 m above mean sea level (AMSL)) over the Pacific Ocean near the coast of California. The air mass was lofted to higher altitudes near the California-Nevada border on 25 January 2010 and remained above 2500 m AMSL until after the sampling period. The mixed depth layer for this same time was below 1000 m AMSL, so the air sampled probably contained aerosol particles that were above the turbulent mixing zone for at least 24 h prior to sampling. RH back trajectories for this same period show that RH levels in the air mass were in excess of 90% near the coast of California. RH gradually decreased as the air was lofted but never dropped below 50%. During the sampling period, HYSPLIT trajectories predict RH levels of 87% at Storm Peak Laboratory, while direct measurements indicate that RH levels were around 97% during the sampling period. Measurements indicate the RH never exceeded 100% during sampling. At high RH most of the hygroscopic aerosol particles sampled would have been deliquesced at the time of sampling [*Martin*, 2000]. The sample for Raman analysis was dried by bringing it to laboratory temperature and RH. After this initial drying, the samples were transported and stored in an RH environment of <30% until the time of experimentation. Hence, we believe the particle sizes given here reflect the dry particle diameters.

Raman: Coarse Mode
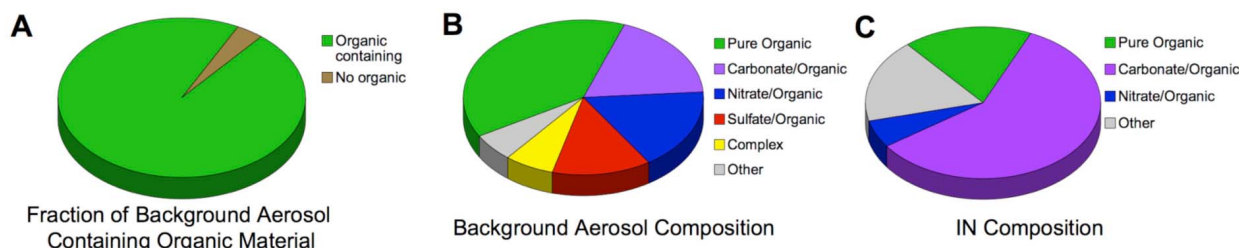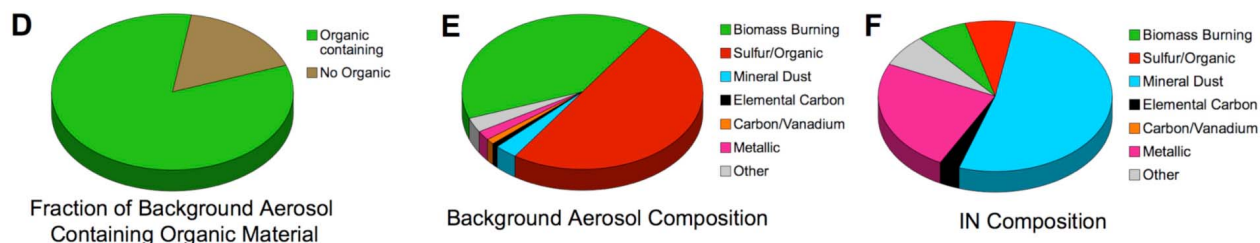

PALMS: Fine Mode

Figure 2. Compositional summary of coarse- and fine-mode aerosol particulate collected at Storm Peak Laboratory using both particle analysis by laser mass spectrometry (PALMS) and Raman analyses. (a, d) The fraction of background aerosol sampled containing some quantity of organic material, including trace amounts, detected using each technique. (b, c, e, f) Particles are classified according to their main constituents, and therefore trace organic species are ignored. However, as demonstrated by Figures 2a and 2d, the majority of the particles (in both background aerosol and ice nuclei (IN) fractions) not classified as "organic only" in Figures 2b, 2c, 2e, and 2f contained a minor organic component or an organic coating.

3.2. Raman Analysis of Coarse-Mode Particulate

[25] Aerosol particles collected in the coarse mode exhibited a wide range of chemical characteristics including organic material, carbonates, sulfates and nitrates. Examination of 175 randomly selected particles revealed that the particles were mainly composed of chemical mixtures in which one of the two main components was organic material. The relative amount of organic material varied from particle to particle and ranged from trace amounts to 100%. As shown in Figure 2a the overwhelming majority (96% ± 2%) of the background particles examined contained organic material. The remaining 4% ± 2% were composed of either pure carbonate-containing minerals or sulfates. Particle composition within the organic-containing particles is shown in Figure 2b. While a significant portion of the particles examined were composed of purely organic material (39% ± 4%), the majority were internally mixed with other species. With the exception of organic material, chemical components generally remained externally mixed with respect to one another. Particles were categorized as complex if they contained more than three distinct chemical species. Only a small subset (7% ± 2%) of the background particles examined were found to be complex mixtures.

[26] Nitrates were detected in 17% ± 3% of the particles. Several other groups have also observed nitrates using Raman spectroscopy for analysis of ambient aerosol particles [Batonneau et al., 2006; Ivleva et al., 2007]. The majority of nitrate detected in this sample had characteristic

Raman peaks matching those of sodium nitrate. Sodium nitrate is indicative of aged salts resulting from heterogeneous reactions of nitric acid on NaCl particles or crustal material [Gard et al., 1998]. Aged salts can be associated with various sources; however, HYSPLIT back trajectories show the sampled air mass at low altitudes near the coast of California which suggests the salts were likely of marine origin. Nitric acid, a product of anthropogenic nitrogen oxide emissions, may have come from urban centers in California when the air mass was at lower altitudes. Sulfates in the coarse-mode sample consisted of ammonium sulfate (7% ± 2%) and other inorganic sulfate-containing salts (6% ± 2%) such as Na_2SO_4 (characteristic Raman frequency 996 cm^{-1}).

[27] The second most prominent particle type observed in the coarse-mode sample was mineral dust or crustal material detected using carbonate as a tracer; this classification may underestimate the total fraction of mineral dust, the chemistry of which varies [Claquin et al., 1999]. For the background particles sampled, 18% ± 3% were found to be carbonate containing. The vast majority were calcium carbonate that was likely produced through primary mechanical processes such as weathering.

[28] Pure organic particles were shown to comprise 39% ± 4% of the background particles sampled. Although the oxidation state of the particles could not be conclusively determined using Raman spectroscopy, the presence or absence of oxygen functional groups was noted. Raman signatures associated with intermolecular hydrogen bonding
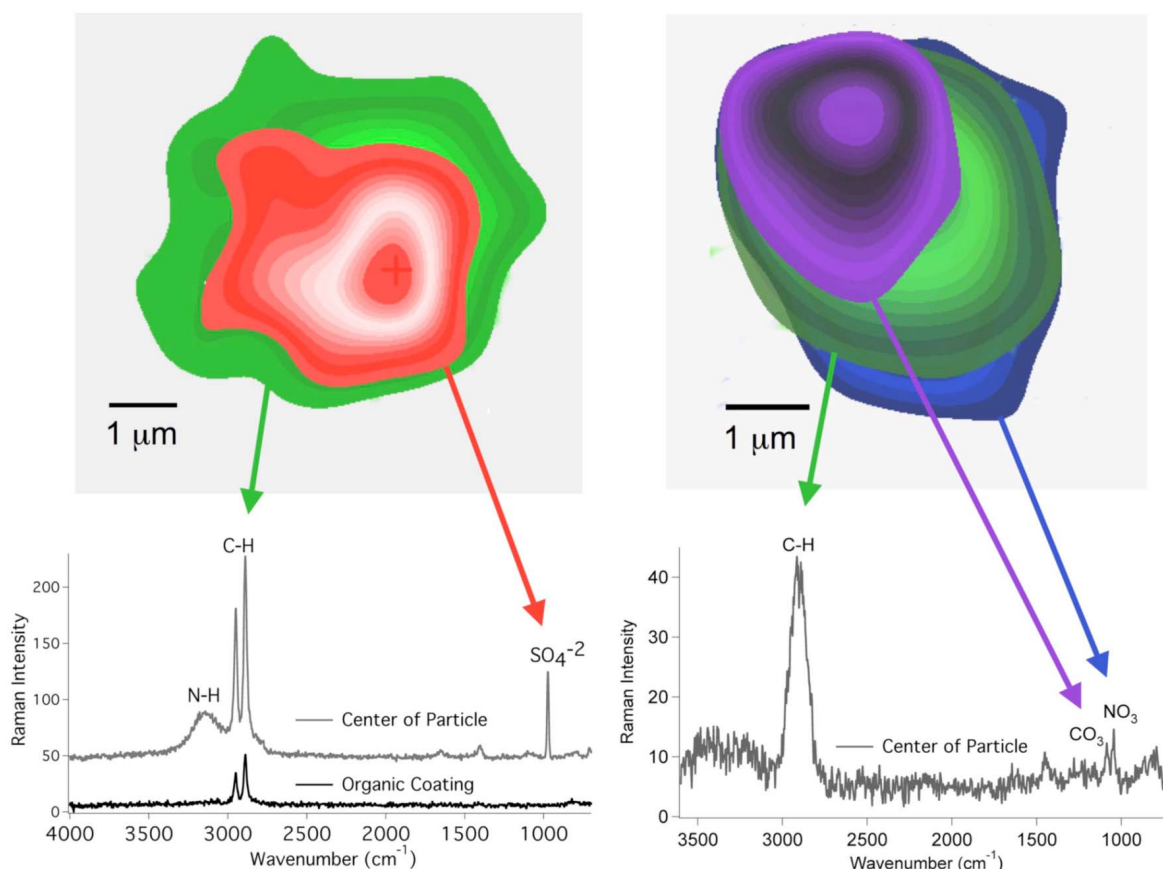
Figure 3. (left) Raman spectral map of an ammonium sulfate particle coated with organic material. The sulfate-containing region is highlighted in red, and organic material is shown in green. (right) A spectral map of a complex uncoated particle with regions containing nitrate (blue) and organics (green) and a smaller region containing a carbonate signature (purple). The spectra shown, with the exception of the organic coating, were obtained near the center of the particle and therefore contain signatures from multiple constituents.

or hydroxyl groups were associated with 24% ± 3% of spectra from background organic particles. Spectra of background aerosol exhibiting a high degree of fluorescence (<6% ± 2%) indicate that some organic compounds consisted of humic substances, high molecular weight aliphatic and aromatic compounds [*Ivleva et al.*, 2007]. Some of the organic particles observed were also visually and spectrally similar to amorphous "tar balls" described by *Posfai et al.* [2003], *Deboudt et al.* [2010], and *Kamphus et al.* [2010]. Tar balls are exclusively found in biomass or biofuel burning emissions. HYSPLIT trajectories indicate that the air mass sampled had been above the turbulent mixing layer for more than 24 h prior to sampling; therefore it is unlikely the sample was affected by wood fire emissions from the town of Steamboat Springs. Tar balls were likely from a source near the coast of California when the air mass was at lower elevations.

3.2.2. Raman Mapping and Particle Coatings

[29] Raman mapping was used to qualitatively determine the location of chemical components within internally mixed particles of interest. Particles were observed with various morphologies and mixing states. Figure 3 provides a visual example of organic-containing particles exhibiting two different morphologies; one is considered coated and the other uncoated. Figure 3 (left) shows a map of a particle that would be considered coated with organic material. The particle core consists of ammonium sulfate (shown in red) that is fully encapsulated by organic material (shown in green). Approximately 15% ± 3% of the particles examined appeared to contain a coating of organic material surrounding an internal core. Organic coatings probably formed because of accumulation of carbonaceous material from both natural and anthropogenic sources via condensation during transport.

[30] For comparison, a map in Figure 3 (right) shows a particle that is not considered coated but contains multiple constituents. This example depicts an aerosol particle of mixed chemical composition; containing organic, carbonate and nitrate Raman signatures. Particle regions containing nitrate are shown in blue and those corresponding to organic material (green) and carbonate (purple) have been layered on top. This particle was categorized as a carbonate-mineral particle that has accumulated organic and nitrate material through condensation.
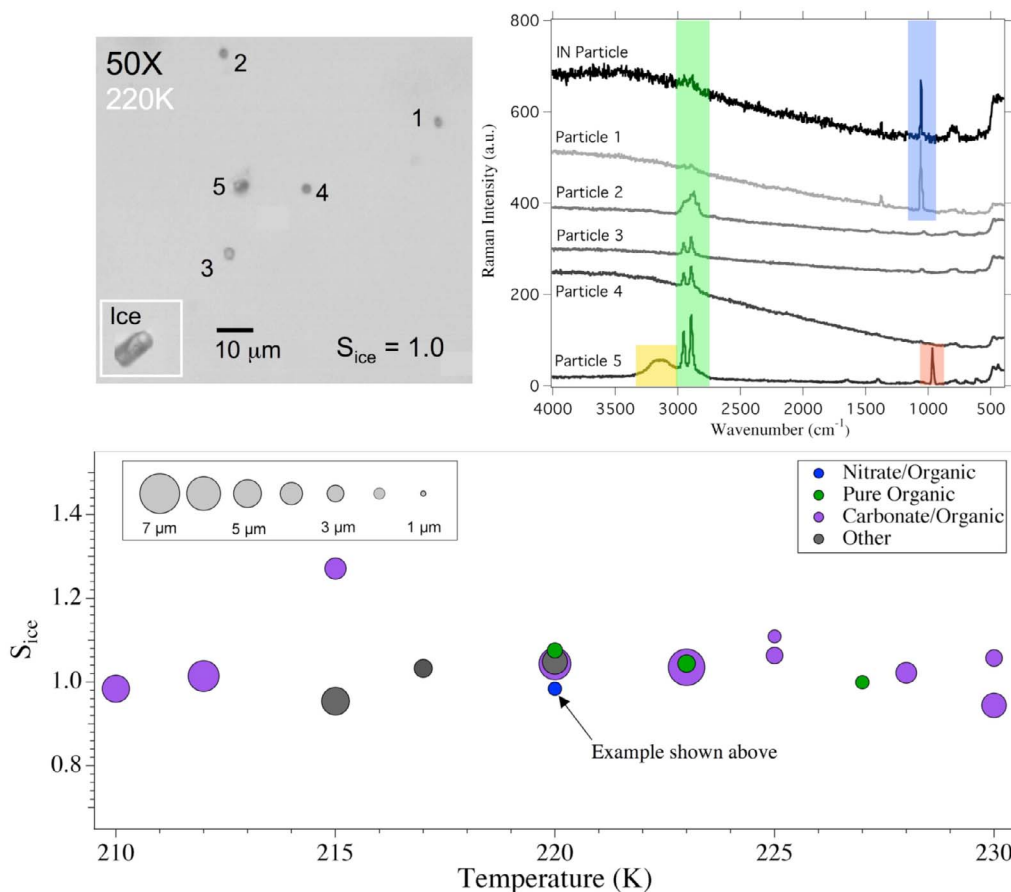
Figure 4. (top) Optical images and spectra obtained during a typical ice nucleation experiment using the Raman system. (right) Spectra have been color blocked to highlight compositional information obtained during the experiment. Peaks associated with the CH stretching of organic material are highlighted in green, ammonium is shown in yellow, and sulfate and nitrate peaks are highlighted in red and blue, respectively. (bottom) A compilation of S_{ice} data obtained from all ice nucleation experiments performed using the coarse-mode sample. S_{ice} data are plotted as a function of temperature, IN size, and composition. Marker size is used to indicate IN size, and composition is denoted by marker color.

3.3. PALMS Analysis of Fine- and Coarse-Mode Particulate

[31] A summary of results obtained from PALMS analysis of fine-mode particulate is shown in Figures 2e–2f. Using the PALMS instrument, mixing state was determined by the presence or absence of a component (e.g., organic species) in the single-particle mass spectra. Using negative ion spectra, the majority (83% ± 3%) of background particles contained organic ions, similar to that observed for the coarse-mode aerosol using Raman spectroscopy. Almost all (∼90%) organic-containing background particles, were either internally mixed sulfate and organic or biomass burning aerosol (Figure 2e), similar to previous measurements (95%) at Storm Peak Laboratory [*DeMott et al.*, 2003]. Particles placed in the biomass burning category were defined as those containing both sulfates and organics, as well as potassium [*Hudson et al.*, 2004]; these particles could be similar to those identified as tar balls using Raman analysis. Elemental carbon, mineral dust and metallic particles each represented less than 2% of the background fine-mode background aerosol by number, similar

to previous measurements at Storm Peak Laboratory [*DeMott et al.*, 2003].

3.4. Ice Nucleation

3.4.1. Results of Raman Ice Nucleation Experiments

[32] A series of laboratory experiments were carried out to examine heterogeneous ice nucleation on the coarse mode sample. Figure 4 (top) shows images and spectra taken during a typical ice nucleation experiment. An optical microscope image taken at 50× magnification (Figure 4, top left) shows the ice crystal that marked the onset of ice formation in the experiment and other non-IN particles that were present in the 50× field of view. The first ice nucleation event observed was used to establish the onset of ice formation. The total number of particles (2162) collected on the coarse-mode sample can be used to estimate the fraction of ice nucleating particles at the onset of ice formation. Assuming the first ice crystal was identified, and that no ice crystals remained undetected outside the field of view, the ice nucleating fraction for these experiments was ∼5 × 10^{-4}. In the example experiment (Figure 4), the onset of freezing was observed at S_{ice} = 1.00 ± 0.05. Spectra
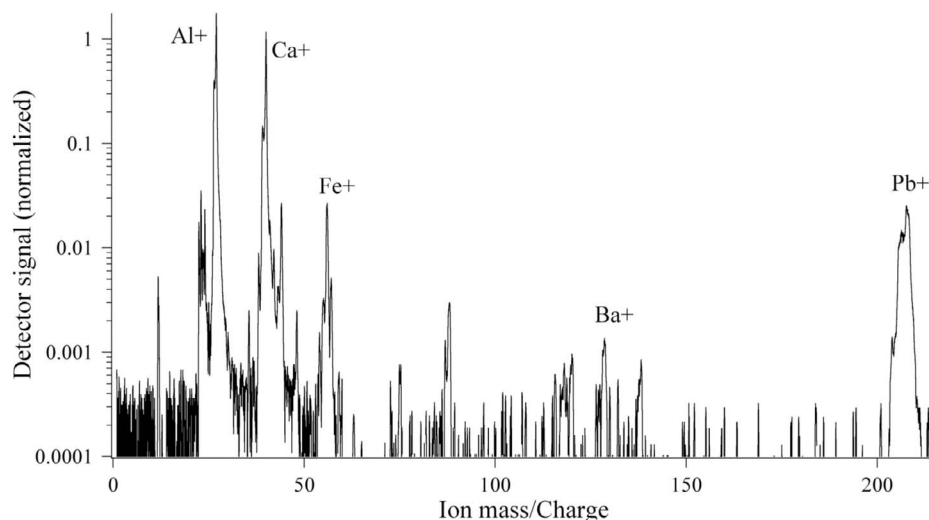
Figure 5. Positive polarity PALMS mass spectrum of a bare mineral dust IN particle. Major peaks include lead, barium, calcium, aluminum, and iron.

corresponding to the IN and other particles in the field of view are shown in Figure 4 (top right). The spectrum of the IN particle contains only a trace organic signature and characteristic peaks associated with sodium nitrate are clearly visible. Particle 1, which did not initiate ice formation, also contained sodium nitrate and trace organic material. Particles 2–4 were classified as purely organic, whereas particle 5 contains ammonium sulfate and organic material. Raman mapping was used to further probe particle 5, and it was found to consist of an ammonium sulfate core surrounded by a coating of organic material (the Raman map of this particle was previously shown as an example of a coated particle in Figure 3).

[33] S_{ice} values calculated for the onset of freezing in each experiment are shown as a function of temperature, relative IN size, and composition in Figure 4 (bottom). IN composition is indicated by marker color and marker size is used to represent IN size. In all cases, ice formation for this sample was observed at low S_{ice} values (average $S_{ice} = 1.04 \pm 0.05$) and was independent of temperature (210 K to 230 K examined). For several experiments in this study ice nucleation was observed at S_{ice} values slightly below, but very close to $S_{ice} = 1.0$. In these instances, S_{ice} values are ≥ 1.0 within the experimental uncertainty of ± 0.05. For experiments performed in this study, IN particles ranged from 2.4 μm to 6.5 μm in size. Average IN diameter was 4.0 ± 1.2 μm, which is not significantly different from the average particle size for the sample (4.0 ± 1.5 μm). A graphical summary of IN composition is shown in Figure 2c. Of the particles that served as IN, the majority were found to be carbonate-containing minerals ($59\% \pm 12\%$). The remaining IN particles were either organic ($18\% \pm 9\%$), nitrate containing ($6\% \pm 6\%$) or of other composition ($18\% \pm 9\%$). Ice was never observed to nucleate on the same particle twice. This could be due to the stochastic nature of ice nucleation or possibly because of microphysical changes in the particles due to ice deposition (deactivation) or repeated heating and freezing of the sample between experiments.

[34] Raman analysis of the coarse-mode IN particles showed they were enriched in minerals and depleted in nitrates and sulfates when compared to the composition of the background aerosol sampled. Observations in this study are consistent with other investigations that have suggested carbonate particles can efficiently nucleate ice [*Manson*, 1957; *Mason and Maybank*, 1958; *Zimmermann et al.*, 2008]. Using environmental scanning electron microscopy combined with energy dispersive x-ray microanalysis, *Klein et al.* [2010] determined that 90% of ambient IN sampled (by electrostatic precipitation) contained either silicate or calcium carbonate material. *Sullivan et al.* [2010] also found that the heterogeneous reaction of nitric acid with calcite and other carbonates tends to inhibit depositional ice formation.

3.4.2. Ice Residue Composition From PALMS

[35] A single-particle mass spectrum of an aerosol particle that heterogeneously nucleated ice in the CIC during the sampling is shown in Figure 5. The positive ion mass spectrum is indicative of a mineral dust particle that has taken up anthropogenic lead [*Murphy et al.*, 2007] and can be a good ice nucleus [*Cziczo et al.*, 2009]. Sulfates and organics are not prevalent; therefore, this particle would generally be considered a bare, or uncoated, mineral dust particle. It should be noted that lead is known to be an easily ionizable substance, and although it is a relatively large peak in this spectrum, laboratory calibrations indicate it accounts for less than 1% of the particle mass [*Murphy et al.*, 2006]. Lead was observed in ~20% of the positive ion mass spectra of IN particles. Since this spectrum came from the largest single IN category, it is considered a representative spectrum.

[36] During the period of interest, IN concentration varied from 1 to 10 per liter, and IN particles ranged in size from 200 to 2000 nm, peaking at ~750 nm (aerodynamic diameter). PALMS analysis of 204 ice residues from the CIC (Figure 2f), show that over three quarters of the IN observed were mineral dust or metallic particles. Mineral dust detected in PALMS spectra largely consisted of aluminosilicate material. Significantly lower abundances of sulfate ($7\% \pm 2\%$) and biomass burning aerosol ($7\% \pm 2\%$) were observed in the ice active fraction than in the background aerosol. Mineral dust and metallic particles were overrepresented in

the ice active aerosol fraction compared to background aerosol composition. These findings are similar to the composition and concentrations of heterogeneous IN previously observed at Storm Peak Laboratory by *DeMott et al.* [2003] and in a follow-up study by *Richardson et al.* [2007]. Mineral dust and fly ash and metallic particles made up the largest proportion of heterogeneous IN in both studies; however, ~25% of the IN were not particles traditionally considered good IN, such as biomass burning particles as well as mixed sulfate and organic particles.

3.4.3. Comparing Raman and PALMS IN Composition

[37] IN particle composition from Raman and PALMS analyses are shown in Figures 2c and 2f, respectively. Organic-containing IN particles (including biomass burning for PALMS analysis) are present in lower percentages than in the background aerosol sampled. Sulfate-organic, metallic and elemental carbon IN are observed in the PALMS analysis but are absent or undetectable in Raman spectra. Nitrate-organic particles were identified by the Raman analysis but not in the PALMS mass spectra. Differences in particle composition observed by each method are well aligned with particle composition expected for the distinct size fractions. For example, over 50% of total atmospheric nitrate by mass is typically found in the coarse mode [*Seinfeld and Pandis*, 1998], which was examined primarily by Raman analysis. Sulfates are often more abundant in smaller particle size fractions [*Wall et al.*, 1988], sampled by PALMS, because they include secondary ammonium sulfate [*Seinfeld and Pandis*, 1998]. Although different information is gathered using each technique and size mode, the general findings are the same. Both techniques found mineral dust or carbonate-containing crustal material enhanced in the IN fraction, while pure organics, organic-containing sulfates, and nitrates were underrepresented compared to concentrations in the background aerosol sampled.

3.4.4. Organic Material Observed in the Ice Active Particle Fraction

[38] Although particles composed purely of organic material were less abundant in the IN fraction compared to the background aerosol sampled, for both size modes organic material was commonly found, in at least trace amounts, in both the background and IN fractions. To further investigate how organic material influences ice nucleation, Raman spectroscopy was used to assess its spatial distribution within individual particles. This analysis showed that organic material was usually present in three distinct ways: in trace amounts, as a coating on the outside of a core particle, or as a particle consisting mainly of organic material.

[39] Organic species present in trace amounts are ubiquitous among sampled IN particles. Using negative ion spectra, PALMS found organic ion fragments (i.e., above the limit of detection) associated with 73% $\pm$ 3% of the ice active particles. Similarly, Raman analysis observed 93% $\pm$ 7% of the IN particles to contain detectable amounts of organic material. These observations are consistent with other studies that have also observed organic material on ambient IN particles. Field measurements by *Pratt et al.* [2009] showed ~60% of mineral dust-containing ice crystal residues associated with humic-like organics and/or biological material. PALMS measurements of subvisible cirrus ice residues by *Froyd et al.* [2010] indicate that internally mixed sulfate-organic particles may heterogeneously

nucleate ice in the tropical tropopause region. Our results are also consistent with laboratory work [*Wise et al.*, 2010] which suggests incomplete organic coatings may leave a particle's core exposed to ambient water vapor which, in turn, can dictate the overall water uptake and ice nucleation ability of the particle. In our experiments, the composition of sampled ice active particles was distinct compared to background aerosol; yet almost every particle contained organic material. This suggests that trace amounts of organic do not heavily influence heterogeneous IN, or we would expect to see a less dramatic composition effect.

[40] Particles containing thick coatings of organic material were identified using Raman spectroscopy, but did not serve as IN. This observation is similar to results presented by *Möhler et al.* [2008], that suggest thick coatings of organic material can inhibit depositional ice nucleation on dust IN. The composition of particle coatings observed by *Möhler et al.* [2008] may, however, be different than coatings observed in the present study, which were generally simple unoxidized aliphatic compounds with spectra similar to the spectrum of organic-coating material shown in Figure 3 (left).

[41] In several Raman experiments, ice formation was observed on particles that were mainly composed of organic material, with no detectable inorganic component. Spectra of these IN particles all contained a broad characteristic Raman peak associated with OH stretching of intermolecular hydrogen bonds (3000–3600 cm^{-1}) or sharper higher-frequency vibrations associated with primary or secondary hydroxyl groups (3250–3650 cm^{-1}). Figure 6 shows three examples of IN spectra exhibiting these features. The broad, low-intensity OH signature seen in the bottom spectrum is not as strong as Raman intensities from water typically observed with particle deliquescence. The observation that the organic IN particles in this study contained oxygen signatures is interesting because, as mentioned previously, the majority of the purely organic particles within the background sample contained no signs of oxygen (~76%). Thus, it is possible that heterogeneous ice nucleation occurs preferentially on organic material that is more highly oxidized.

[42] Past studies of ice nucleation on oxidized organic material offer several possible explanations for this observation. Recent work by *Knopf et al.* [2010] provides evidence that anthropogenic aerosol particles, consisting mainly of organics, can act as sufficient IN under cirrus-forming conditions. *Fukuta* [1966] investigated the ice nucleation threshold temperature of 329 different organic species that were exclusively low-solubility, crystalline solids with high melting points. Every organic compound also possessed polar or hydrogen-bonding groups. *Fukuta* [1966] found no simple relationship between molecular shape and ice nucleation; however, suitable compounds for ice nucleation often had surface sites available for hydrogen bonding. There are only a few previous studies examining the role of gas phase oxidation and ice nucleation. Oxidation by ozone does not significantly alter the IN ability of soot particles [*Dymarska et al.*, 2006; *Friedman et al.*, 2011]. *Wang and Knopf* [2011] investigated ice nucleation on humic-like substances before and after exposure to ozone. Results indicated oxidation could either promote or inhibit heterogeneous ice nucleation depending on the substance.
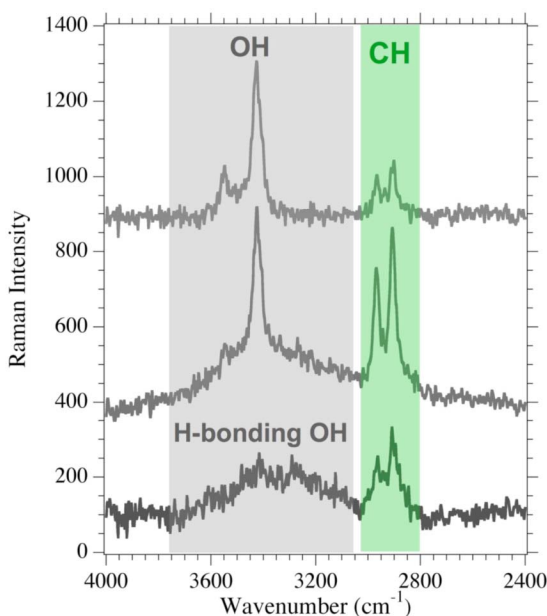
Figure 6. Raman spectra obtained from three IN particles that consisted of mainly organic material. All have oxygen signatures associated with their spectra. The weak broad OH peak between 3000 and 3600 cm^{-1} (bottom spectrum) is indicative of intermolecular hydrogen bonding. This spectral feature is similar to OH signatures observed for glassy oxygenated organic material [*Tong et al.*, 2011] but is much weaker than the OH intensity associated with water during particle deliquescence.

[43] Some organic compounds may form noncrystalline solids known as glasses. *Zobrist et al.* [2008] have shown that some soluble organics, and multiple component solutions, can form glassy solids at atmospherically relevant temperatures <230 K. *Virtanen et al.* [2010] have also observed solid-like behavior of naturally occurring secondary organic aerosol particles at ambient air temperatures. Such highly viscous organic glasses may act as surfaces for heterogeneous ice formation in cirrus as well [*Murray et al.*, 2010]. Given the temperature range used for Raman investigation in this study, it is possible that oxygenated organic particles observed as IN particles were glassy or highly viscous in nature.

[44] The precise reason that oxygenated organics were observed as IN in this study, however, remains unclear. Studies are needed to determine whether oxidized organic material can serve as more efficient IN than unoxidized organics and to determine the physical or chemical explanation for this phenomenon. We find the relationship between ice formation and organic material is not straightforward. It seems that organic material can serve to either promote or inhibit heterogeneous ice formation depending on its chemical composition and the spatial distribution of chemicals in internally mixed particles.

4. Conclusions

[45] Chemical composition of ambient background aerosol and IN were investigated through experiments using Raman spectroscopy and mass spectra gathered using an inline CIC and PALMS instrument. In both coarse and fine aerosol modes, minerals dust particles were overrepresented, and nitrate and sulfates were underrepresented in the ice-nucleating aerosol fraction, compared to abundances of the same species in background aerosol sampled. Trace organic material was found ubiquitously in both the ambient and ice-nucleating aerosol fractions. The Raman technique was used to provide new insights into the role of organics in ice nucleation. Purely organic particles that nucleated ice in Raman experiments all contained evidence of oxidation. We speculate these particles were glassy (or highly viscous) in nature or that the presence of oxygen may have influenced the ice nucleation ability of these particles. Particles that consisted of an inner core material and nonoxygenated organic coating were not observed as IN particles. Results presented suggest that heterogeneous ice nucleation on organic material cannot be generalized and may depend on both chemical composition and particle morphology. This relationship should be investigated further.

References

Baranska, H., A. Labudzinzka, and J. Terpinski (1987), *Laser Raman Spectrometry: Analytical Applications*, 271 pp., Halsted, New York.

Batonneau, Y., S. Sobanska, J. Laureyns, and C. Bremard (2006), Confocal microprobe Raman imaging of urban tropospheric aerosol particles, *Environ. Sci. Technol.*, *40*(4), 1300–1306, doi:10.1021/es051294x.

Baustian, K. J., M. E. Wise, and M. A. Tolbert (2010), Depositional ice nucleation on solid ammonium sulfate and glutaric acid particles, *Atmos. Chem. Phys.*, *10*(5), 2307–2317, doi:10.5194/acp-10-2307-2010.

Blaha, J. J., and G. J. Rosasco (1978), Raman microprobe spectra of individual microcrystals and fibers of talc, tremolite, and related silicate minerals, *Anal. Chem.*, *50*(7), 892–896, doi:10.1021/ac50029a018.

Borys, R. D., and M. A. Wetzel (1997), Storm Peak Laboratory: A research, teaching, and service facility for the atmospheric sciences, *Bull. Am. Meteorol. Soc.*, *78*(10), 2115–2123, doi:10.1175/1520-0477(1997) 078<2115:SPLART>2.0.CO;2.

Buck, A. L. (1981), New equations for computing vapor-pressure and enhancement factor, *J. Appl. Meteorol.*, *20*(12), 1527–1532, doi:10.1175/ 1520-0450(1981)020<1527:NEFCVP>2.0.CO;2.

Cantrell, W., and A. Heymsfield (2005), Production of ice in tropospheric clouds: A review, *Bull. Am. Meteorol. Soc.*, *86*(6), 795–807, doi:10.1175/BAMS-86-6-795.

Chou, C., O. Stetzer, E. Weingartner, Z. Juranyi, Z. A. Kanji, and U. Lohmann (2011), Ice nuclei properties within a Saharan dust event at the Jungfraujoch in the Swiss Alps, *Atmos. Chem. Phys.*, *11*(10), 4725–4738, doi:10.5194/ acp-11-4725-2011.

Claquin, T., M. Schulz, and Y. J. Balkanski (1999), Modeling the mineralogy of atmospheric dust sources, *J. Geophys. Res.*, *104*(D18), 22,243–22,256, doi:10.1029/1999JD900416.

Coleyshaw, E. E., G. Crump, and W. P. Griffith (2003), Vibrational spectra of the hydrated carbonate minerals ikaite, monohydrocalcite, lansfordite and nesquehonite, *Spectrochim. Acta, Part A*, *59*(10), 2231–2239.

Cziczo, D. J., P. J. DeMott, C. Brock, P. K. Hudson, B. Jesse, S. M. Kreidenweis, A. J. Prenni, J. Schreiner, D. S. Thomson, and D. M. Murphy (2003), A method for single particle mass spectrometry

of ice nuclei, *Aerosol Sci. Technol.*, 37(5), 460–470, doi:10.1080/02786820300976.

Cziczo, D. J., D. M. Murphy, P. K. Hudson, and D. S. Thomson (2004), Single particle measurements of the chemical composition of cirrus ice residue during CRYSTAL-FACE, *J. Geophys. Res.*, 109, D04201, doi:10.1029/2003JD004032.

Cziczo, D. J., D. S. Thomson, T. L. Thompson, P. J. DeMott, and D. M. Murphy (2006), Particle analysis by laser mass spectrometry (PALMS) studies of ice nuclei and other low number density particles, *Int. J. Mass Spectrom.*, 258(1–3), 21–29, doi:10.1016/j.ijms.2006.05.013.

Cziczo, D. J., et al. (2009), Inadvertent climate modification due to anthropogenic lead, *Nat. Geosci.*, 2(5), 333–336, doi:10.1038/ngeo499.

Deboudt, K., P. Flament, M. Choel, A. Gloter, S. Sobanska, and C. Colliex (2010), Mixing state of aerosols and direct observation of carbonaceous and marine coatings on African dust by individual particle analysis, *J. Geophys. Res.*, 115, D24207, doi:10.1029/2010JD013921.

DeMott, P. J., D. C. Rogers, and S. M. Kreidenweis (1997), The susceptibility of ice formation in upper tropospheric clouds to insoluble aerosol components, *J. Geophys. Res.*, 102(D16), 19,575–19,584, doi:10.1029/97JD01138.

DeMott, P. J., D. J. Cziczo, A. J. Prenni, D. M. Murphy, S. M. Kreidenweis, D. S. Thomson, R. Borys, and D. C. Rogers (2003), Measurements of the concentration and composition of nuclei for cirrus formation, *Proc. Natl. Acad. Sci. U. S. A.*, 100(25), 14,655–14,660, doi:10.1073/pnas.2532677100.

DeMott, P. J., A. J. Prenni, X. Liu, S. M. Kreidenweis, M. D. Petters, C. H. Twohy, M. S. Richardson, T. Eidhammer, and D. C. Rogers (2010), Predicting global atmospheric ice nuclei distributions and their impacts on climate, *Proc. Natl. Acad. Sci. U. S. A.*, 107(25), 11,217–11,222, doi:10.1073/pnas.0910818107.

Dymarska, M., B. J. Murray, L. M. Sun, M. L. Eastwood, D. A. Knopf, and A. K. Bertram (2006), Deposition ice nucleation on soot at temperatures relevant for the lower troposphere, *J. Geophys. Res.*, 111, D04204, doi:10.1029/2005JD006627.

Freedman, M. A., K. J. Baustian, M. E. Wise, and M. A. Tolbert (2010), Characterizing the morphology of organic aerosols at ambient temperature and pressure, *Anal. Chem.*, 82(19), 7965–7972, doi:10.1021/ac101437w.

Friedman, B., G. Kulkarni, J. Beránek, A. Zelenyuk, J. Thornton, and D. Cziczo (2011), Ice nucleation and droplet formation by bare and coated soot particles, *J. Geophys. Res.*, 116, D17203, doi:10.1029/2011JD015999.

Froyd, K. D., D. M. Murphy, P. Lawson, D. Baumgardner, and R. L. Herman (2010), Aerosols that form subvisible cirrus at the tropical tropopause, *Atmos. Chem. Phys.*, 10(1), 209–218, doi:10.5194/acp-10-209-2010.

Fukuta, N. (1966), Experimental studies of organic ice nuclei, *J. Atmos. Sci.*, 23(2), 191–196, doi:10.1175/1520-0469(1966)023<0191:ESOOIN>2.0.CO;2.

Fung, K. H., and I. N. Tang (1992), Analysis of aerosol-particles by resonance Raman-scattering technique, *Appl. Spectrosc.*, 46(1), 159–162, doi:10.1366/0003702924444399.

Fung, K. H., and I. N. Tang (1999), chemical characterization of aerosol particles by laser Raman spectroscopy, in *Aerosol Chemical Processes in the Environment*, edited by K. R. Spurny and D. Hochrainer, pp. 177–195, CRC Press, Boca Raton, Fla.

Gard, E. E., et al. (1998), Direct observation of heterogeneous chemistry in the atmosphere, *Science*, 279(5354), 1184–1187, doi:10.1126/science.279.5354.1184.

Gierens, K. (2003), On the transition between heterogeneous and homogeneous freezing, *Atmos. Chem. Phys.*, 3, 437–446, doi:10.5194/acp-3-437-2003.

Guedes, A., N. Ribeiro, H. Ribeiro, M. Oliveira, F. Noronha, and I. Abreu (2009), Comparison between urban and rural pollen of *Chenopodium alba* and characterization of adhered pollutant aerosol particles, *J. Aerosol Sci.*, 40(1), 81–86, doi:10.1016/j.jaerosci.2008.07.012.

Hallar, A. G., G. Chirokova, I. B. McCubbin, T. H. Painter, C. Wiedimyer, and C. Dodson (2011), Atmospheric bioaerosols transported via dust storms in western United States, *Geophys. Res. Lett.*, 38, L17801, doi:10.1029/2011GL048166.

Hudson, P. K., D. M. Murphy, D. J. Cziczo, D. S. Thomson, J. A. de Gouw, C. Warneke, J. Holloway, J. R. Jost, and G. Hubler (2004), Biomass-burning particle measurements: Characteristic composition and chemical processing, *J. Geophys. Res.*, 109, D23S27, doi:10.1029/2003JD004398.

Intergovernmental Panel on Climate Change (2007), *Climate Change 2007: The Physical Science Basis. Contribution of Working Group I to the Fourth Assessment Report of the Intergovernmental Panel on Climate Change*, edited by S. Solomon et al., Cambridge Univ. Press, Cambridge, U. K.

Ivleva, N. P., U. McKeon, R. Niessner, and U. Poschl (2007), Raman microspectroscopic analysis of size-resolved atmospheric aerosol particle

samples collected with an ELPI: Soot, humic-like substances, and inorganic compounds, *Aerosol Sci. Technol.*, 41(7), 655–671, doi:10.1080/02786820701376391.

Kamphus, M., M. Ettner-Mahl, T. Klimach, F. Drewnick, L. Keller, D. J. Cziczo, S. Mertes, S. Borrmann, and J. Curtius (2010), Chemical composition of ambient aerosol, ice residues and cloud droplet residues in mixed-phase clouds: Single particle analysis during the Cloud and Aerosol Characterization Experiment (CLACE 6), *Atmos. Chem. Phys.*, 10(16), 8077–8095, doi:10.5194/acp-10-8077-2010.

Kärcher, B. (2005), Supersaturation, dehydration, and denitrification in Arctic cirrus, *Atmos. Chem. Phys.*, 5, 1757–1772, doi:10.5194/acp-5-1757-2005.

Klein, H., et al. (2010), Saharan dust and ice nuclei over Central Europe, *Atmos. Chem. Phys.*, 10, 10,211–10,221, doi:10.5194/acp-10-10211-2010.

Knopf, D. A., and T. Koop (2006), Heterogeneous nucleation of ice on surrogates of mineral dust, *J. Geophys. Res.*, 111, D12201, doi:10.1029/2005JD006894.

Knopf, D. A., B. Wang, A. Laskin, R. C. Moffet, and M. K. Gilles (2010), Heterogeneous nucleation of ice on anthropogenic organic particles collected in Mexico City, *Geophys. Res. Lett.*, 37, L11803, doi:10.1029/2010GL043362.

Koop, T., B. P. Luo, A. Tsias, and T. Peter (2000), Water activity as the determinant for homogeneous ice nucleation in aqueous solutions, *Nature*, 406(6796), 611–614, doi:10.1038/35020537.

Kulkarni, G., M. Pekour, A. Afchine, D. M. Murphy, and D. J. Cziczo (2011), Comparison of experimental and numerical studies of the performance characteristics of a pumped counterflow virtual impactor, *Aerosol Sci. Technol.*, 45(3), 382–392, doi:10.1080/02786826.2010.539291.

Lin-Vien, D., N. B. Colthup, W. G. Fateley, and J. G. Grasselli (1991), *Infrared and Raman Characteristic Frequencies of Organic Molecules*, 503 pp., Academic, San Diego, Calif.

Manson, J. E. (1957), Calcium carbonate as an ice nucleus, *J. Meteorol.*, 14(1), 85–86, doi:10.1175/0095-9634-14.1.85.

Marti, J., and K. Mauersberger (1993), A survey and new measurements of ice vapor-pressure at temperatures between 170 and 250K, *Geophys. Res. Lett.*, 20(5), 363–366, doi:10.1029/93GL00105.

Martin, S. T. (2000), Phase transitions of aqueous atmospheric particles, *Chem. Rev.*, 100(9), 3403–3454, doi:10.1021/cr990034t.

Mason, B. J., and J. Maybank (1958), Ice-nucleating properties of some natural mineral dusts, *Q. J. R. Meteorol. Soc.*, 84(361), 235–241, doi:10.1002/qj.49708436104.

Mikkelsen, A., A. B. Andersen, S. B. Engelsen, H. C. B. Hansen, O. Larsen, and L. H. Skibsted (1999), Presence and dehydration of ikaite, calcium carbonate hexahydrate, in frozen shrimp shell, *J. Agric. Food Chem.*, 47(3), 911–917, doi:10.1021/jf980932a.

Möhler, O., S. Benz, H. Saathoff, M. Schnaiter, R. Wagner, J. Schneider, S. Walter, V. Ebert, and S. Wagner (2008), The effect of organic coating on the heterogeneous ice nucleation efficiency of mineral dust aerosols, *Environ. Res. Lett.*, 3(2), 025007, doi:10.1088/1748-9326/3/2/025007.

Mund, C., and R. Zellner (2003), Freezing nucleation of levitated single sulfuric acid/H$_2$O micro-droplets: A combined Raman- and Mie spectroscopic study, *J. Mol. Struct.*, 661–662, 491–500, doi:10.1016/j.molstruc.2003.08.034.

Murphy, D. M., D. J. Cziczo, K. D. Froyd, P. K. Hudson, B. M. Matthew, A. M. Middlebrook, R. E. Peltier, A. Sullivan, D. S. Thomson, and R. J. Weber (2006), Single-particle mass spectrometry of tropospheric aerosol particles, *J. Geophys. Res.*, 111, D23S32, doi:10.1029/2006JD007340.

Murphy, D. M., et al. (2007), Distribution of lead in single atmospheric particles, *Atmos. Chem. Phys.*, 7(12), 3195–3210, doi:10.5194/acp-7-3195-2007.

Murray, B. J., et al. (2010), Heterogeneous nucleation of ice particles on glassy aerosols under cirrus conditions, *Nat. Geosci.*, 3(4), 233–237, doi:10.1038/ngeo817.

Nyquist, R. A., C. L. Putzig, A. M. Leugers, and R. O. Kagel (1997), *The Handbook of Infrared and Raman Spectra of Inorganic Compounds and Organic Salts*, 1184 pp., Academic, San Diego, Calif.

Obrist, D., A. G. Hallar, I. McCubbin, B. B. Stephens, and T. Rahn (2008), Atmospheric mercury concentrations at Storm Peak Laboratory in the Rocky Mountains: Evidence for long-range transport from Asia, boundary layer contributions, and plant mercury uptake, *Atmos. Environ.*, 42(33), 7579–7589, doi:10.1016/j.atmosenv.2008.06.051.

Pekour, M. S., and D. J. Cziczo (2011), Wake capture, particle breakup, and other artifacts associated with counterflow virtual impaction, *Aerosol Sci. Technol.*, 45(6), 758–764, doi:10.1080/02786826.2011.558942.

Posfai, M., R. Simonics, J. Li, P. V. Hobbs, and P. R. Buseck (2003), Individual aerosol particles from biomass burning in southern Africa: 1. Compositions and size distributions of carbonaceous particles, *J. Geophys. Res.*, 108(D13), 8483, doi:10.1029/2002JD002291.

Potgieter-Vermaak, S. S., and R. Van Grieken (2006), Preliminary evaluation of micro-Raman spectrometry for the characterization of individual aerosol particles, *Appl. Spectrosc.*, 60(1), 39–47, doi:10.1366/000370206775382848.

Pratt, K. A., P. J. DeMott, J. R. French, Z. Wang, D. L. Westphal, A. J. Heymsfield, C. H. Twohy, A. J. Prenni, and K. A. Prather (2009), In situ detection of biological particles in cloud ice-crystals, *Nat. Geosci.*, 2(6), 398–401, doi:10.1038/ngeo521.

Pruppacher, H. R., and J. D. Klett (1997), *Microphysics of Clouds and Precipitation*, Kluwer Acad., Norwell, Mass.

Ren, C., and A. R. Mackenzie (2005), Cirrus parametrization and the role of ice nuclei, *Q. J. R. Meteorol. Soc.*, 131(608), 1585–1605, doi:10.1256/qj.04.126.

Richardson, M. S., et al. (2007), Measurements of heterogeneous ice nuclei in the western United States in springtime and their relation to aerosol characteristics, *J. Geophys. Res.*, 112, D02209, doi:10.1029/2006JD007500.

Rosasco, G. J., E. S. Etz, and W. A. Cassatt (1975), Analysis of discrete fine particles by Raman-spectroscopy, *Appl. Spectrosc.*, 29(5), 396–404, doi:10.1366/000370275774455752.

Sadezky, A., H. Muckenhuber, H. Grothe, R. Niessner, and U. Poschl (2005), Raman micro spectroscopy of soot and related carbonaceous materials: Spectral analysis and structural information, *Carbon*, 43(8), 1731–1742, doi:10.1016/j.carbon.2005.02.018.

Santachiara, G., L. Di Matteo, F. Prodi, and F. Belosi (2010), Atmospheric particles acting as ice forming nuclei in different size ranges, *Atmos. Res.*, 96(2–3), 266–272, doi:10.1016/j.atmosres.2009.08.004.

Seinfeld, J. H., and S. N. Pandis (1998), *Atmospheric Chemistry and Physics: From Air Pollution to Climate Change*, 1326 pp., John Wiley, New York.

Sobanska, S., G. Falgayrac, J. Laureyns, and C. Bremard (2006), Chemistry at level of individual aerosol particle using multivariate curve resolution of confocal Raman image, *Spectrochim. Acta, Part A*, 64(5), 1102–1109.

Spichtinger, P., and D. J. Cziczo (2010), Impact of heterogeneous ice nuclei on homogeneous freezing events in cirrus clouds, *J. Geophys. Res.*, 115, D14208, doi:10.1029/2009JD012168.

Spichtinger, P., and K. M. Gierens (2009a), Modelling of cirrus clouds—Part 2: Competition of different nucleation mechanisms, *Atmos. Chem. Phys.*, 9(7), 2319–2334, doi:10.5194/acp-9-2319-2009.

Spichtinger, P., and K. M. Gierens (2009b), Modelling of cirrus clouds—Part 1a: Model description and validation, *Atmos. Chem. Phys.*, 9(2), 685–706, doi:10.5194/acp-9-685-2009.

Spichtinger, P., and K. M. Gierens (2009c), Modelling of cirrus clouds—Part 1b: Structuring cirrus clouds by dynamics, *Atmos. Chem. Phys.*, 9(2), 707–719, doi:10.5194/acp-9-707-2009.

Stetzer, O., B. Baschek, F. Luond, and U. Lohmann (2008), The Zurich Ice Nucleation Chamber (ZINC)—A new instrument to investigate atmospheric ice formation, *Aerosol Sci. Technol.*, 42(1), 64–74, doi:10.1080/02786820701787944.

Sullivan, R. C., L. Minambres, P. J. DeMott, A. J. Prenni, C. M. Carrico, E. J. T. Levin, and S. M. Kreidenweis (2010), Chemical processing does not always impair heterogeneous ice nucleation of mineral dust particles, *Geophys. Res. Lett.*, 37, L24805, doi:10.1029/2010GL045540.

Tang, I. N., and K. H. Fung (1989), Characterization of inorganic salt particles by Raman-spectroscopy, *J. Aerosol Sci.*, 20(5), 609–617, doi:10.1016/0021-8502(89)90106-7.

Tong, H. J., J. P. Reid, D. L. Bones, B. P. Luo, and U. K. Krieger (2011), Measurements of the timescales for the mass transfer of water in glassy aerosol at low relative humidity and ambient temperature, *Atmos. Chem. Phys.*, 11(10), 4739–4754, doi:10.5194/acp-11-4739-2011.

Uzu, G., S. Sobanska, Y. Aliouane, P. Pradere, and C. Dumat (2009), Study of lead phytoavailability for atmospheric industrial micronic and submicronic particles in relation with lead speciation, *Environ. Pollut.*, 157(4), 1178–1185, doi:10.1016/j.envpol.2008.09.053.

Virtanen, A., et al. (2010), An amorphous solid state of biogenic secondary organic aerosol particles, *Nature*, 467(7317), 824–827, doi:10.1038/nature09455.

Wall, S. M., W. John, and J. L. Ondo (1988), Measurement of aerosol size distributions for nitrate and major ionic species, *Atmos. Environ.*, 22(8), 1649–1656, doi:10.1016/0004-6981(88)90392-7.

Wang, B. B., and D. A. Knopf (2011), Heterogeneous ice nucleation on particles composed of humic-like substances impacted by O_3, *J. Geophys. Res.*, 116, D03205, doi:10.1029/2010JD014964.

Wise, M. E., K. J. Baustian, and M. A. Tolbert (2010), Internally mixed sulfate and organic particles as potential ice nuclei in the tropical tropopause region, *Proc. Natl. Acad. Sci. U. S. A.*, 107(15), 6693–6698, doi:10.1073/pnas.0913018107.

Yeung, M. C., and C. K. Chan (2010), Water content and phase transitions in particles of inorganic and organic species and their mixtures using micro-Raman spectroscopy, *Aerosol Sci. Technol.*, 44(4), 269–280, doi:10.1080/02786820903583786.

Zimmermann, F., S. Weinbruch, L. Schutz, H. Hofmann, M. Ebert, K. Kandler, and A. Worringen (2008), Ice nucleation properties of the most abundant mineral dust phases, *J. Geophys. Res.*, 113, D23204, doi:10.1029/2008JD010655.

Zobrist, B., C. Marcolli, D. A. Pedernera, and T. Koop (2008), Do atmospheric aerosols form glasses?, *Atmos. Chem. Phys.*, 8(17), 5221–5244, doi:10.5194/acp-8-5221-2008.

K. J. Baustian and M. A. Tolbert, Cooperative Institute for Research in Environmental Sciences, University of Colorado Boulder, Boulder, CO 80309, USA. (baustian@colorado.edu)

D. J. Cziczo, Department of Earth, Atmospheric and Planetary Sciences, Massachusetts Institute of Technology, Cambridge, MA 02139, USA.

A. G. Hallar, Storm Peak Laboratory, Desert Research Institute, PO Box 882530, Steamboat Springs, CO 80488, USA.

G. Kulkarni, Pacific Northwest National Laboratory, PO Box 999, Richland, WA 99352, USA.

K. A. Pratt, Department of Chemistry, Purdue University, West Lafayette, IN 47907, USA.

M. E. Wise, Department of Chemistry, Concordia University, Portland, OR 97211, USA.